Quaternized 1,2,3-Triazolyl Content and Modulation Potentiate Antibacterial and Antifungal Activities of Amphipathic Peptoids

Cassandra Guerinot, Mélodie Malige, Kathakali De, Marc Maresca, Nicolas Charbonnel, Elise Courvoisier-Dezord, Nicolas Vidal, Olivier Roy, Frederic Laurent, Jérôme Josse, et al.

▶ **To cite this version:**

Cassandra Guerinot, Mélodie Malige, Kathakali De, Marc Maresca, Nicolas Charbonnel, et al.. Quaternized 1,2,3-Triazolyl Content and Modulation Potentiate Antibacterial and Antifungal Activities of Amphipathic Peptoids. ACS Infectious Diseases, 2024, 10.1021/acsinfecdis.4c00591 . hal-04749560

HAL Id: hal-04749560
https://uca.hal.science/hal-04749560v1

Submitted on 23 Oct 2024

HAL is a multi-disciplinary open access archive for the deposit and dissemination of scientific research documents, whether they are published or not. The documents may come from teaching and research institutions in France or abroad, or from public or private research centers.

L'archive ouverte pluridisciplinaire **HAL**, est destinée au dépôt et à la diffusion de documents scientifiques de niveau recherche, publiés ou non, émanant des établissements d'enseignement et de recherche français ou étrangers, des laboratoires publics ou privés.

Author Submitted Version

Published version via this link: https://doi.org/10.1021/acsinfecdis.4c00591

Quaternized 1,2,3-triazolyl content and modulation potentiate anti-bacterial and anti-fungal activity of amphipathic peptoids

Cassandra Guerinot,[a] Mélodie Malige,[b] Kathakali De,[c] Marc Maresca,[d] Nicolas Charbonnel,[b] Elise Courvoisier-Dezord,[d] Nicolas Vidal,[e] Olivier Roy,[a] Frederic Laurent,[f] Jérôme Josse,[f] Christopher Aisenbrey,[c] Burkhard Bechinger,[c] Christiane Forestier,[b*] Sophie Faure[a*]

[a] Université Clermont Auvergne, Clermont Auvergne INP, CNRS, ICCF, F-63000 Clermont−Ferrand, France. Corresponding author Email: sophie.faure@uca.fr

[b] Université Clermont Auvergne, CNRS, LMGE, F-63000 Clermont−Ferrand, France Corresponding author Email: christiane.forestier@uca.fr

[c] Université de Strasbourg, CNRS, Institut de Chimie, F-67008 Strasbourg, France

[d] Aix Marseille Univ, CNRS, Centrale Med, ISM2, 13013, Marseille, France

[e] Yelen Analytics, Aix-Marseille University ICR, 13013 Marseille, France.

[f] CIRI – Centre International de Recherche en Infectiologie, Inserm, U1111, Université Claude Bernard Lyon 1, CNRS, UMR5308, Ecole Normale Supérieure de Lyon, Univ Lyon, F-69007, Lyon, France

Abstract :

Bioinspired from cationic antimicrobial peptides, sequence-defined triazolium-grafted peptoid oligomers (6- to 12-mer) were designed to adopt an amphipathic helical polyproline I-type structure. Their evaluation on a panel of bacterial strains (*Escherichia coli*, *Pseudomonas aeruginosa*, *Staphylococcus aureus*, *Enterococcus faecalis*), pathogenic fungi (*Candida albicans*, *Cryptococcus neoformans*, *Aspergillus fumigatus*) and human cells (hRBC, BEAS-2B, Caco-2, HaCaT, HepG2) enabled to identify two heptamers with improved activity to selectively fight *Staphylococcus aureus* pathogens. Modulation of parameters, such as the nature of the triazolium and hydrophobic/lipophilic side chains, the charge content and the sequence length, drastically potentiates activity and selectivity. Besides, the ability to block the pro-inflammatory effect induced by lipopolysaccharide or lipoteichoic acid was

also explored. Finally, biophysical studies by circular dichroism and fluorescence spectroscopies strongly supported that the bactericidal effect of these triazolium-grafted oligomers was primarily due to the selective disruption of the bacterial membrane.

Keywords : antimicrobial, antifungal, peptidomimetic, triazolium, selectivity, membrane permeability

Antimicrobial peptides (AMPs) exhibit broad-spectrum activity against various pathogens (bacteria, fungi, viruses). They are also referred as host defense peptides (HDPs) to highlight they are part of the innate immune system of all multicellular organisms, and often associated with immunomodulatory effect.[1] Their mechanism of action involves first the interaction with the cytoplasmic membrane of prokaryotic cells leading to permeabilization or perturbation of the bacterial membrane, and/or translocation to interact with internal targets to affect cell processes.[2,3] Due to their rapid and multitarget bactericidal effect, HDPs are now considered a potential alternative to classical antibiotics for tackling the global problem of antibioresistance.[4] However, the direct use of these natural peptides as therapeutics is hampered principally by low metabolic stability, poor pharmacokinetics, residual toxicity and also costly synthesis scale-up. To overcome these inherent drawbacks, research efforts are devoted to the development of modified peptides and peptidomimetics that are easier to synthesize, less toxic and more stable. In this context, the design of antimicrobial peptidomimetic foldamers, *i.e.* synthetic sequence-specific oligomers mimicking peptide and able to fold in well-defined three-dimensional structure, is particularly pertinent.[5,6] Indeed, the HDPs folding is a key determinant for the selective interaction with the prokaryotic cell membranes, in particular those exhibiting cationic amphipathic structure such as cecropin and magainin.[7,8] Through electrostatic interactions, a certain degree of selectivity is achieved because bacterial membranes rich in acidic phospholipids are more negatively charged than those of mammalian cells. Different types of helix-stabilized peptidomimetic foldamers including modified α-peptides, β-peptides, γ-peptides, oligoureas and peptoids, have been developed to mimic cationic amphipathic AMPs with great potential in term of antimicrobial activities, selectivity and stability.[6,9,10] Peptoid (*i.e. N*-alkyl glycine oligomer) foldamers have been particularly

scrutinized since the report from Barron's group in 2003 on peptoids (12-17-mer) exhibiting PolyProline-I (PPI) type helical structure with potent antibacterial activity against both Gram-positive (*Bacillus subtilis*) and Gram-negative (*Escherichia coli*) bacteria.[11] The influence of charge distribution, hydrophobic content, sequence length and nature of the side-chains on the antimicrobial activity and the cell selectivity for prokaryotes over eukaryotes has been intensively studied in order to find the right balance between potency and toxicity.[12,13,14,15] Encouraging results were obtained thanks to the shortening of the sequence and optimization of hydrophobic side-chains.[16,17,18] Besides, cyclisation of oligomers and modulation of helicity were also found to be key factors.[19, 20] Less studied is the nature of the cationic groups. We recently showed that classical primary ammonium and guanidinium moieties can be advantageously replaced by triazolium groups.[21,22] Indeed, short peptoid oligomers incorporating triazolium-type side chain as cationic groups exhibited antibacterial activities on Gram-positive bacterial strains *Staphylococcus aureus* and *Enterococcus faecalis* similar to longer oligomers but with much less toxicity. It is therefore important to deepen the study of peptoid oligomers carrying quaternized 1,2,3-triazolyl side chains to better understand the key elements of their structure responsible for their antibacterial activity and selectivity.

In this study, several series of short triazolium-grafted peptoid oligomers were designed to exhibit cationic amphipathic character upon structuration into a PPI-type helix. We anticipated that modulation of quaternized 1,2,3-triazolyl groups (nature and number) could enable the optimization of the potency and the selectivity. This study explored the spectrum of activity of this type of peptoid oligomers against panel of Gram-positive and Gram-negative bacterial strains and pathogenic fungi, their selectivity for prokaryotic cells (*i.e.* their low cytotoxicity against human cells) and their potential anti-inflammatory activity. The link between three-dimensional structuration of triazolium-grafted oligomers and their membrane activity was studied using circular dichroism and fluorescent leakage assay.

RESULTS

Design and synthesis of the triazolium-grafted oligopeptoids. A panel of oligomers from hexamers to dodecamers was designed to exhibit amphipathic structures through the formation of PPI-type helix, typical secondary structure of peptoids featuring *cis*-amide bond geometry along the backbone.[23] Typically, the periodic incorporation of a cationic side chain every three residues, the remaining positions being occupied by hydrophobic side chains, allows the formation of cationic amphipathic helical structure. The propensity to fold into PPI-type helix depends mainly on the propensity of the backbone amides to adopt a *cis* conformation, the sequence length and a preferred sense of helicity imposed by the side chains chirality. Many side chains have been developed to induce the cis amide conformation,[24] in particular α-chiral aromatic or aliphatic side chains but also triazolium-type side chains that are among the most effective.[25] Therefore, only cis-directing side chains were employed to design the sequences: different quaternized 1,2,3-triazolyl (t^+) as cationic groups and two type of hydrophobic α-chiral side chains (H): the aromatic (S)-1-phenyl ethyl (spe) and the aliphatic (S)-1-tert-butyl ethyl (stbe) (Figure 1, table 1).

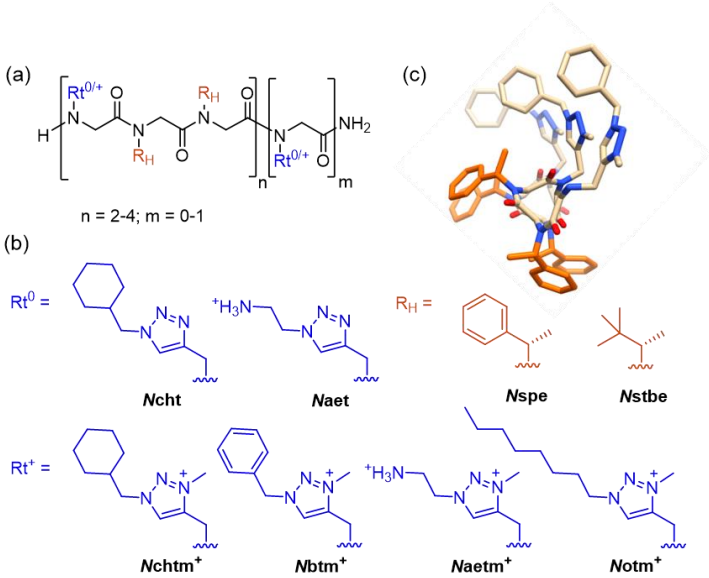

Figure 1. Triazole- and triazolium-grafted peptoid oligomers design: (a) Generic structure of the studied oligomers; (b) Nature of the side-chains and abbreviations[26] and (c) Top view of a model structure of the heptamer H-*N*chtm$^+$-*N*spe-*N*spe-*N*chtm$^+$-*N*spe-*N*spe-*N*chtm$^+$-NH_2 **A-3** using backbone dihedral angles values of the peptoid PPI-type helix (ω 0, ϕ -75, φ 170).

All peptoid oligomers were synthesized using a solid-phase strategy developed to access peptoid oligomers featuring triazolium-type side chains.[21] The synthetic pathway involved a modified protocol of the classical solid-phase submonommer method for sequence elongation using different primary amines[27] followed by post-modification of all propargyl side chains into triazolium by a Huisgen reaction/methylation sequence (Scheme 1; ESI for details).

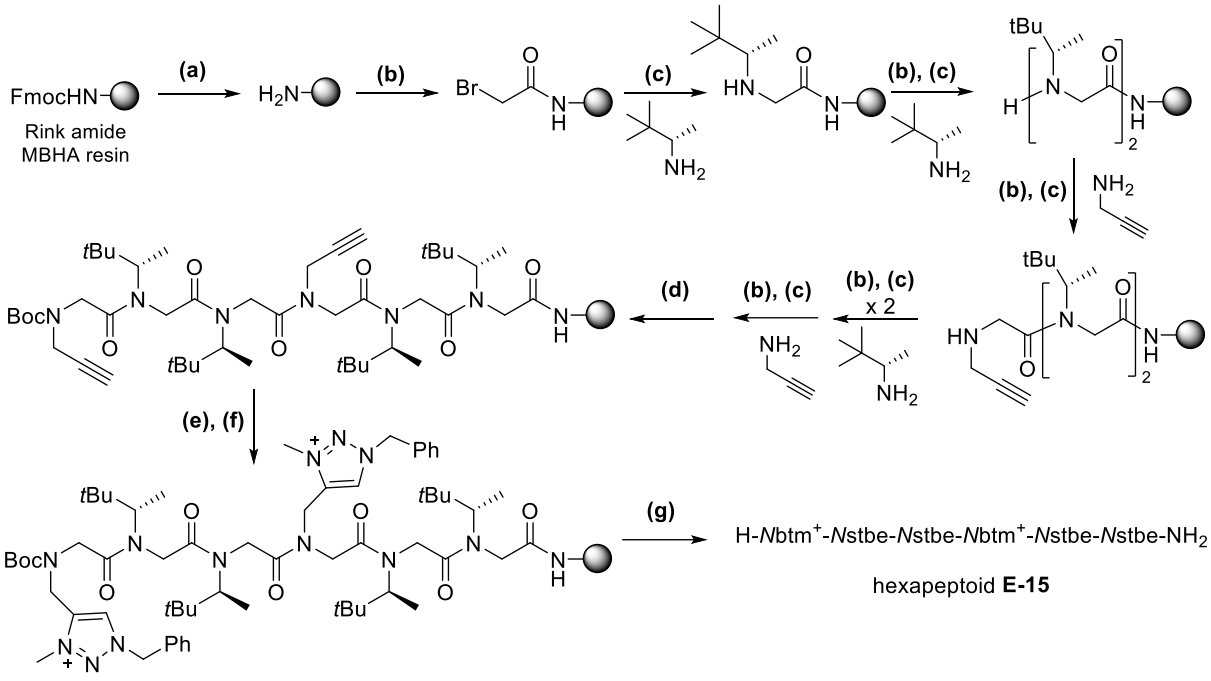

Scheme 1. General procedure to access triazolium-based peptoid oligomers illustrated by the synthesis of the hexamer H-*N*btm$^+$-*N*stbe-*N*stbe-*N*btm$^+$-*N*stbe-*N*stbe-NH_2 **E-15**. Key conditions: (a) Fmoc deprotection: Piperidine (20% in DMF), 15 min; (b) Acylation step: $BrCH_2CO_2H$ (6 equiv., 0.4 M in DMF), DIC (8 equiv., 2 M in DMF), 40°C, 5 min; (c) Substitution step: (S)-1-tert-butyl ethylamine or propargylamine (25 equiv., 2 M in DMF), 40°C, 1h; (d) Boc_2O (6 equiv.), DIPEA (12 equiv.), DMF, 40°C, 1h; (e) CuAAc reaction: BnN_3 (4 equiv. per alkyne group), ascorbic acid (6 equiv.), CuI (12 equiv.), DIPEA (15 equiv.), DMF/Pyridine (7:3), rt, overnight; (f) Methylation: CH_3I (neat), 45°C, overnight; (g) Cleavage from the resin: TFA/triisopropylsilane/water (95:2.5:2.5 by volume), rt, 30 min.

Peptoids from 6-mer to 12-mer (**1**-**17**) with cationic charge ranging from 0 to 8 were obtained with good to excellent analytical high performance liquid chromatography (HPLC) purity after purification (Table 1). Each oligomer was characterized using high performance liquid chromatography-mass spectrometry (LC-MS) and high-resolution mass spectrometry (HRMS).

Table 1. Sequences of designed triazole- and triazolium-based peptoids

Series	Cpd Nb	Sequences[a]	Length	Charge	HPLC purity[b] (%)	HPLC Retention time[d]	Exact mass
A	**1**	H-*N*cht-*N*spe-*N*spe-*N*cht-*N*spe-*N*spe-NH_2	6-mer	0	90	9.58	1130.6648
	2	H-*N*chtm$^+$-*N*spe-*N*spe-*N*chtm$^+$-*N*spe-*N*spe-NH_2	6 mer	+2	95	8.86	579.8528
	3	H-*N*chtm$^+$-*N*spe-*N*spe-*N*chtm$^+$-*N*spe-*N*spe-*N*chtm$^+$-NH_2	7-mer	+3	97	8.60	469.6258
	4	H-*N*chtm-*N*spe-*N*spe-*N*chtm-*N*spe-*N*spe-*N*chtm-*N*spe-*N*spe-NH_2	9-mer	0	91	10.49	843.9948
	5	H-*N*chtm$^+$-*N*spe-*N*spe-*N*chtm$^+$-*N*spe-*N*spe-*N*chtm$^+$-*N*spe-*N*spe-NH_2	9-mer	+3	94	9.10	577.0155
B	**6**	H-*N*btm$^+$-*N*spe-*N*spe-*N*btm$^+$-*N*spe-*N*spe-NH_2	6-mer	+2	95	8.45	573.8055
	7	H-*N*btm$^+$-*N*spe-*N*spe-*N*btm$^+$-*N*spe-*N*spe-*N*btm$^+$-NH_2	7-mer	+3	97	8.60	463.5782
	8	H-*N*btm$^+$-*N*spe-*N*spe-*N*btm$^+$-*N*spe-*N*spe-*N*btm$^+$-*N*spe-*N*spe-NH_2	9-mer	+3	95	8.68	570.9681
C	**9**	H-*N*aetm$^+$-*N*spe-*N*spe-*N*aetm$^+$-*N*spe-*N*spe-NH_2	6-mer	+4	97	7.35	526.8004
	10	H-*N*aetm$^+$-*N*spe-*N*spe-*N*aetm$^+$-*N*spe-*N*spe-*N*aetm$^+$-*N*spe-*N*spe-NH_2	9-mer	+6	94	7.14	523.9631
	11	H-*N*aetm-*N*spe-*N*spe-*N*aetm-*N*spe-*N*spe-*N*aetm-*N*spe-*N*spe-*N*aetm-*N*spe-*N*spe-NH_2	12-mer	+4	90	7.52	678.0348
	12	H-*N*aetm$^+$-*N*spe-*N*spe-*N*aetm$^+$-*N*spe-*N*spe-*N*aetm$^+$-*N*spe-*N*spe-*N*aetm$^+$-*N*spe-*N*spe-NH_2	12-mer	+8	94	7.52	522.7946
D	**13**	H-*N*otm$^+$-*N*spe-*N*spe-*N*otm$^+$-*N*spe-*N*spe-NH_2	6-mer	+2	91	9.50	595.8822
	14	H-*N*otm$^+$-*N*spe-*N*spe-*N*otm$^+$-*N*spe-*N*spe-*N*otm$^+$-NH_2	7-mer	+3	95	8.77	485.6561
E	**15**	H-*N*btm$^+$-*N*stbe-*N*stbe-*N*btm$^+$-*N*stbe-*N*stbe-NH_2	6-mer	+2	91[c]	8.27	533.8678
	16	H-*N*btm$^+$-*N*stbe-*N*stbe-*N*btm$^+$-*N*stbe-*N*stbe-*N*btm$^+$-NH_2	7-mer	+3	94[c]	7.90	436.9538
	17	H-*N*btm$^+$-*N*stbe-*N*stbe-*N*btm$^+$-*N*stbe-*N*stbe-*N*btm$^+$-*N*stbe-*N*stbe-NH_2	9-mer	+3	91[c]	8.34	531.0294

[a]Peptoid monomers nomenclature in reference 26; [b]HPLC purity at 214 nm; [c]Purity validated by LC-MS, HRMS and ^{1}H NMR. [d]Analytical HPLC performed on a AGILENT 1100 series coupled to DAD detector equipped with an NUCLEODUR 100-3 (C18, 125 mm, Ø 4.6 mm) with a flow of 1 mL/min using solvent A: water (0.1% TFA) and solvent B: MeCN with the following gradient: 5% B (0-2 min), 5→95% B (2-9 min), 95% B (9-12 min).

Antibacterial activity against a panel of ESKAPE pathogens and hemolytic activity. We first screened these triazole- and triazolium-grafted peptoid oligomers (**1**-**17**) on a panel of representative Gram-negative strains (*Escherichia coli* JM109 and ATCC25922, *Pseudomonas aeruginosa* ATCC27853) and Gram-positive strains (*Staphylococcus aureus* CIP6525, *Enterococcus faecalis* ATCC29212) (Table 2). A general trend of selectivity for bacterial *versus* mammalian cells was rapidly assessed by testing the

hemolytic activity on human red blood cells (hRBC) of the compounds exhibiting antimicrobial activities.

Table 2. Antibacterial and hemolytic activities (expressed in μM) of the triazole- and triazolium-grafted peptoids

	E.coli JM109	***E.coli ATCC25922***	***P.aeruginosa ATCC27853***	***E.faecalis ATCC29212***	***S.aureus CIP6525***	**hRBC** [b]	**Selectivity ratio**[d]
Series-Cpds	MIC/MBC [a]	MIC/MBC[a]	MIC/MBC[a]	MIC/MBC[a]	MIC/MBC[a]	HC_{50} [c]	$HC50/MIC_{S.a}$
A-1	>100/>100	>100/>100	>200/>200	>100/>100	>100/>100	-	-
A-2	50/50	50/50	>200/>200	6.3/12.5	3.1/6.3	79.5+/-4.9	25.6
A-3	12.5/25	12.5/12.5	100/100	3.2/6.25	1.6/1.6	66.9+/-6.1	41.8
A-4	>100/>100	>100/>100	>200/>200	>100/>100	>100/>100	>100	-
A-5	25/25	25/25	166/>200	1.8/3.1	1.6/6.3	5.3+/-4.2	3.3
B-6	100/>100	>100/>100	>100/>100	50/100	3.2/6.25	>100	>31.2
B-7	25/25	25/100	>100/>100	16.7/25	3.2/3.2	>100	>31.2
B-8	12.5/25	12.5/25	>200/>200	1.6/3.2	1.6/3.2	33.8+/-11.1	21.1
C-9	>100/>100	>100/>100	>200/>200	>100/>100	>100/>100	>100	-
C-10	25/50	100/>200	>200/>200	50/100	50/100	>100	>2
C-11	6.3/12.5	12.5/25	37.5/50	11.5/25	10.4/12.5	>100	>9.6
C-12	11.5/12.5	50/100	33/50	6.3/12,5	6.3/12.5	55.0+/-8.8	8.7
D-13	25/25	25/25	50/50	6.25/12.5	3.2/6.25	10.3+/-7.4	3.2
D-14	25/25	12.5/12.5	50/50	6.25/6.25	12.5/12.5	4.1+/-6.2	0.3
E-15	>100/>100	100/100	>100/>100	12.5/12.5	1.6/3.2	68.6+/-7.4	42.9
E-16	50/100	25/25	>100/>100	12.5/25	1.6/3.2	>100	>62.5
E-17	50/50	25/25	100/100	1.6/1.6	1.6/1.6	9.1+/-13.7	5.7
Melittin[e]	6.3/12.5	6.3/12.5	12.5/25	6.3/12.5	3.1/6.3	-	-

[a]Minimum inhibitory concentration (MIC) and minimum bactericidal concentration (MBC) are mean values of three independent experiments; [b]human red blood cells; [c]Hemolytic concentration HC_{50} values (*i.e.* the concentrations causing 50% hemolysis) were calculated using GraphPad® Prism 7 software from dose-dependent toxicity curves (see ESI). Results are expressed in means +/- SD (n=3); [d]Selectivity ratio (SR) is calculated as following: $HC_{50}/MIC_{S.aureus}$; [e]Honey bee peptide GIGAVLKVLTTGLPALISWIKRKRQQ used as reference.

From the series **A** (peptoids **1**-**5** composed of *N*spe as hydrophobic residues and triazoles/triazoliums carrying cyclohexyl group *N*chtm/*N*chtm+), it was clear that the presence of the cationic triazolium side-chains was necessary to obtain bacterial activity. Indeed, triazole precursors **1** and **4**, showed no effect towards Gram-negative or Gram-positive pathogens while the triazolium derivatives **2** and **5** exhibited modest activity on *E. coli* and high activities against Gram-positive strains, particularly *S. aureus* (MIC 3.1 and 1.6 μM, respectively). It was noteworthy that an increase in the antibacterial activity was observed across the whole panel when an additional triazolium-based residue was added

in *C*-terminal position of hexamer **2** leading to heptamer **3**. But, the hemolytic activity only slightly increased, therefore a great increase in the selectivity ratio (SR) was observed (25.6 for **2** versus 41.8 for **3**). By contrast, the nonamer **5** comprising three repeats of the triazolium-hydrophobic-hydrophobic (t^+HH) motif exhibited similar antibacterial activities but a dramatic increase in the hemolytic activity with a SR collapsing to 3.3. In the second series **B** (peptoids **6-8** composed of *N*spe as hydrophobic residues and triazoliums carrying benzyl group *N*btm+), the same trend was observed when increasing the sequence length but the increase in hemolytic activity for the nonamer **8** was less marked than for nonamer **6** (HC_{50} 33.8 versus 5.3 μM). A totally different behavior was observed for series **C** (peptoids **9**-**12** composed of *N*spe as hydrophobic residues and triazoles/triazoliums carrying aminoethyl group *N*aetm/*N*aetm+). Triazolium-based hexamer **9** showed no effect on the panel of pathogens and nonamer **10** a very low activity against *E. coli*, *E. faecalis* and *S. aureus.* No hemolytic activity was detected at this sequence length, it was therefore decided to evaluate longer oligomers. The triazole-based dodecamer **11** showed broad spectrum activity with MIC ranging from 37.5 μM for *P. aeruginosa* to 6.3 μM for *E. coli* JM109 and HC_{50} superior to 100 μM. The triazolium-based dodecamer **12** exhibited similar activities but reverse selectivity for Gram-positive bacteria compared to dodecamer **11** and highest hemolytic activity. Oligomers from series **D** (peptoids **13-14** composed of *N*spe as hydrophobic residues and triazoliums carrying octyl group *N*otm+) were found to have a broader spectrum of activity at short length than oligomers of series **A** and **B**. Indeed, hexamer **13** had effect on the panel of Gram-negative bacteria even *P. aeruginosa,* a trend not observed for hexamers of other series. By contrast, no real beneficial was observed through addition of a triazolium-based residue in *C*-terminal position (hexamer **13** versus heptamer **14**). Unfortunately, the strong hemolytic activities of series **D** oligomers were detrimental to their potential interest. The last series **E** (peptoids **15-17** composed of *N*stbe as hydrophobic residues and triazoliums carrying benzyl group *N*btm+) could be directly compared to series **B** in order to highlight the influence of the chiral aliphatic (*S*)-tert-butylethyl (stbe) *versus* the chiral aromatic (*S*)-phenylethyl (spe) as hydrophobic side chains. The hexamer **E-15** showed slightly better antibacterial activity against Gram-positive strains than hexamer

B-6 but also an increase in the hemolytic effect (HC_{50} of 68.6 compared to >100 μM). However, the selectivity ratio remained interesting with a value above 40. Heptamer **E-16** has the same activity profile as heptamer **B-7** with improved selectivity for *S. aureus* thus leading to a higher selectivity ratio, greater than 60. Again, increasing the sequence length to the nonamer resulted in a decrease in selectivity for bacteria versus red blood cells with a SR value of 5.7.

Antifungal activity. The antifungal effect of 14 selected peptoid oligomers was tested against three pathogenic fungi: the yeasts *Candida albicans* (DSM 10697), *Cryptococcus neoformans* (DSM 11959) and the filamentous fungi *Aspergillus fumigatus* (DSM 819) and compared to the hemolytic activity also reported in table 3.

Table 3. Antifungal and hemolytic activities of the triazole- and triazolium-grafted peptoids

	C. albicans	***C. neoformans***	***A. fumigatus***	**hRBC**[b]
Series-Cpds	MIC/MFC[a]	MIC/MFC [a]	MIC/MFC[a]	HC_{50}[c]
A-2	50/50	50/50	100/100	79.5+/-4.9
A-3	18.7/25	12.5/12.5	50/50	66.9+/-6.1
A-4	>100/>100	>100/>100	>100/>100	>100
A-5	4.7/6.2	3.1/6.2	6.2/12.5	5.3+/-4.2
B-6	75/100	50/50	>100/>100	>100
B-8	12.5/12.5	9.4/12.5	25/25	33.8+/-11.1
C-9	>100/>100	>100/>100	>100/>100	>100
C-10	37.5/50	12.5/25	>100/>100	>100
C-12	12.5/12.5	4.7/6.2	100/>100	55.0+/-8.8
D-13	3.1/3.1	3.1/3.1	4.7/6.2	10.3+/-7.4
D-14	1.6/3.1	1.6/3.1	3.1/6.2	4.1+/-6.2
E-15	100/100	50/100	75/100	68.6+/-7.4
E-16	37.5/50	25/25	>100/>100	>100
E-17	18.7/25	6.2/12.5	25/25	9.1+/-13.7
Ampho B	0.7/0.7	0.3/0.3	1.9/1.9	-
Fluconazol	7.8/62.5	25/>100	>100/>100	-

[a]Minimum inhibitory concentration (MIC) and Minimum Fungicidal Concentration (MFC) are expressed in μM and are mean values of experiments conducted in duplicate (n = 2); [b]human red blood cells; [c]HC_{50} values expressed in μM and reported from Table 2.

Uncharged triazole-based nonamer **4** from **A** series and hexamer **9** from **C** series had no effect on selected fungi. In each series, a significant improvement of the MIC for the panel of fungi was observed by increasing the sequence length from hexamer to nonamer. For example, in series A, hexamer **2** exhibited low activity against *C. albicans* (MIC 50 μM) while the heptamer **3** proved slightly better (MIC

18.7 μM) and a MIC value of 4.7 μM was reached with nonamer **5**. Unfortunately, high level of hemolysis was detected for nonamer **5** with HC_{50} value closed to the MIC value. Same selectivity profiles were observed for nonamer **8** (series **B**), and nonamer **17** (series **E**). By contrast, nonamer **10** from the C series was not hemolytic but had also lower antifungal activities. No activity was observed on *A. fumigatus* and MIC values of 37.5 and 12.5 μM on *C. albicans* and *C. neoformans*, respectively. However, an interesting antifungal effect on *C. neoformans* was observed for dodecamer **12** exhibiting a MIC more than 10 times lower than the HC_{50} (4.7 versus 55). Finally, it was worth noting that the short **D**-series oligomers, hexamer **13** and heptamer **14** showed potent antifungal activities against all tested fungi with MICs ranging from 4.7 to 1.6 μM but as mentioned previously, these oligomers carrying an octyl group were highly hemolytic despite their short length.

Toxicity evaluation on a panel of representative cell lines. The toxicity of selected oligomers for a panel of human cells was evaluated using resazurin assay according described protocols.[28] The following representative human cell types: BEAS-2B (normal human bronchial epithelial cell line), Caco-2 (human intestinal epithelial cell line), HaCaT (normal human keratinocytes) and HepG2 (human liver cell line) were subjected to each peptoid oligomer. CC_{50} values (*i.e.* the concentrations of peptoid causing 50% reduction of the cell viability) were determined for each cell lines (Table 4).

Table 4. Cytotoxic concentrations of the peptoids on human cells

Peptoids	**CC_{50}[a]**				**HC_{50}[b]**
Series-Cpds	**BEAS-2B**	**Caco-2**	**HaCaT**	**HepG2**	**hRBC**
A-2	64.9+/-4.1	59.1+/-2.8	38.9+/-2.5	73.4+/-3.9	79.5+/-4.9
A-3	65.4+/-4.3	55.2+/-3.7	26.1+/-5.1	59.5+/-6.6	66.9+/-6.1
A-4	>100	>100	>100	>100	>100
A-5	10.1+/-3.8	7.9+/-3.7	4.8+/-2.7	25.9+/-4.3	5.3+/-4.2
B-6	69.7+/-8.1	74.1+/-3.8	63.5+/-2.1	>100	>100
B-7	>100	94.0+/-2.3	>100	>100	>100
B-8	36.9+/-1.5	15.8+/-2.9	13.1+/-2.2	40.2+/-3.8	33.8+/-11.1
C-9	>100	>100	>100	>100	>100
C-10	97.7+/-4.4	98.5+/-3.4	94.9+/-7.8	>100	>100
C-12	67.3+/-5.7	60.8+/-4.5	58.5+/-3.2	67.1+/-5.2	55.0+/-8.8
D-13	17.1+/-3.1	12.5+/-4.2	5.6+/-3.1	22.8+/-5.2	10.3+/-7.4
D-14	8.1+/-0.9	6.3+/-5.1	2.9+/-3.4	17.6+/-2.7	4.1+/-6.2
E-15	51.9+/-3.6	57.5+/-7.7	30.6+/-2.0	71.2+/-4.4	68.6+/-7.4
E-16	45.9+/-3.6	63.0+/-5.2	56.4+/-3.8	62.5+/-5.7	>100

E-17	3.9+/-0.5	8.1+/-3.5	4.3+/-2.3	17.4+/-3.8	9.1+/-13.7

[a]CC_{50} values (*i.e.* the concentrations causing 50% reduction of the cell viability) are expressed in μM; [b]HC_{50} values are expressed in μM and reported from Table 2.

The general trend was consistent with hemolytic activities previously mentioned. Indeed, peptoids **A-4, B-6, B-7, C-9, C-10** and **E-16** exhibiting a HC_{50} superior to 100 μM, revealed the lowest level of toxicity over the panel of cell lines. Correspondingly, the most hemolytic oligomers **A-5, B-8, D-13, D-14** and **E-17** were found the most cytotoxic ones. Triazolium-grafted nonamers **5**, **8** and **17** from series **A, B** and **E**, respectively, revealed particularly cytotoxic again showing that increasing the length of the oligomer was detrimental to the selectivity. By contrast, nonamer **10** from series **C** exhibited very low toxicity with CC_{50} in between 95 (HaCaT) to >100 μM (HepG2) and dodecamer **12** from this series was still less toxic than nonamers from other series. Most oligomers showed different levels of toxicity depending on cell lines. Normal human keratinocyte cell lines were found to be the more susceptible cells to peptoid exposure.

Anti-inflammatory activity. The ability of these triazole/triazolium-based peptoids to block the pro-inflammatory effect induced by lipopolysaccharide (LPS) or lipoteichoic acid (LTA) was explored. To this aim, the inhibitory activity of peptoids and polymyxin B (PMB, reference compound) against LPS and LTA was assessed using eLUCidate™ Raw 264.7 NF-κB reporter cell line (AMSBIO) as previously described.[29] Inhibitory concentrations IC_{50} on LPS and LTA-induced inflammation were reported and compared to the concentrations causing 50% reduction of the cell viability (Figure 2; ESI).

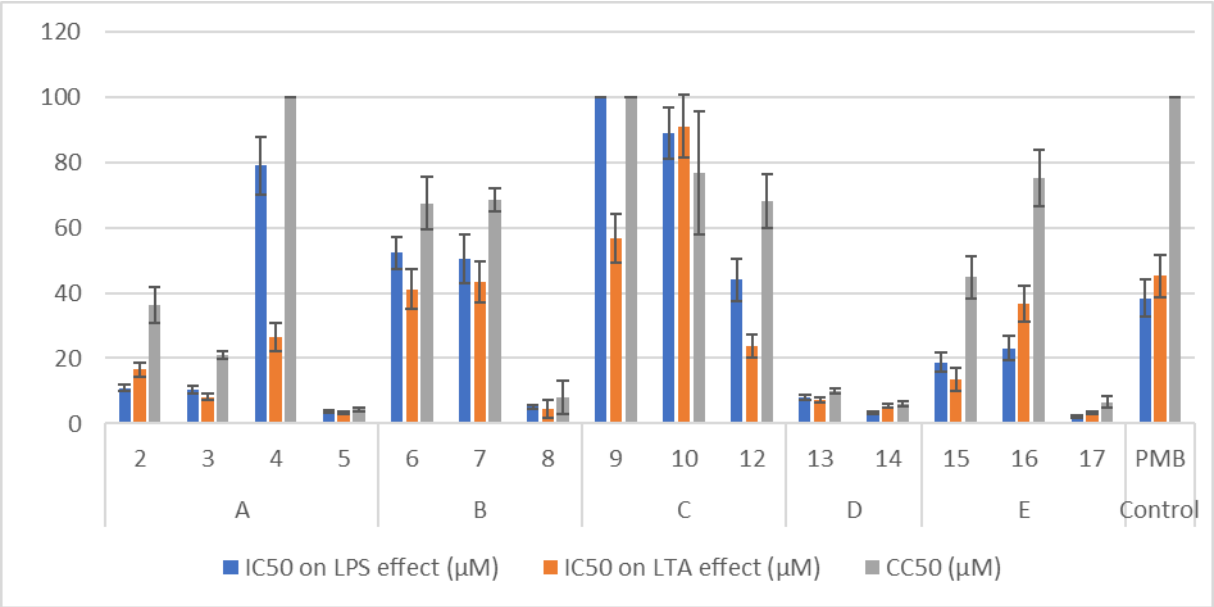

Figure 2. Inhibitory concentrations of peptoids on LPS and LTA-induced inflammation evaluated on eLUCidate™ Raw 264.7 NF-κB reporter cells.

Regarding the inflammation caused by the LPS from *E. coli* or the LTA from *S. aureus*, interesting IC_{50} < 10 µM were obtained for peptoids **A-5**, **B-8, D-13**, **D-14** and **E-17** with no preference for LPS or LTA-mediated inflammation. However, these results cannot be uncorrelated with a cytotoxic effect since the concentrations causing 50% reduction of the viability of Raw 264.7 NF-κB reporter cells were in the same range of values. Peptoids **B-6** and **B-7** showed similar modest effects on LPS and LTA (IC_{50} ≈ 40-50 µM) but also associated with decreased reporter cells viability (CC_{50} ≈ 70 µM). By contrast, peptoids **A-4**, **C-9**, **C-12**, **E-15** and **E-16** seemed to show a noticeable anti-inflammatory effect when considering cytotoxicity. Among them, oligomers **A-4**, **C-9** and **C-12** appeared more active on LTA-mediated inflammation than LPS-mediated one, while oligomers **E-15** and **E-16**, as polymyxin B, showed no selectivity for the two inflammatory stimuli.

Structural study using circular dichroism with bacterial model membrane. To monitor the membrane interactions of peptoids, the concomitant changes in their secondary structure were followed by circular dichroism (CD) spectroscopy by comparing the peptoid spectra in presence and absence of lipid vesicles mimicking bacterial or eukaryotic membranes, respectively (Figure 3). For this study, two

representative peptoid oligomers were selected: peptoid **A-3** which was one of the most potent on the panel of bacterial strains and the inactive peptoid **C-9**.

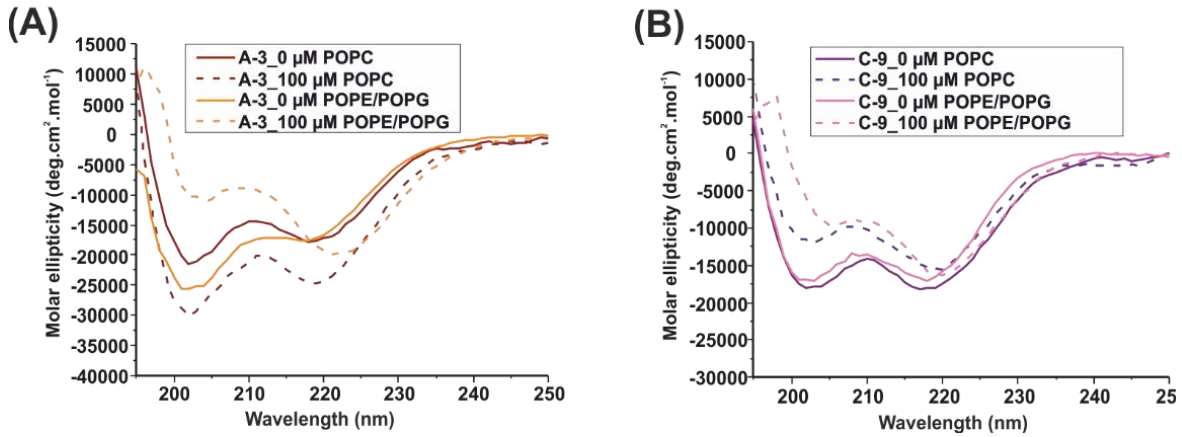

Figure 3. Circular dichroism of (A) peptoid **A-3** and (B) peptoid **C-9** in the absence (bold line) and presence (dotted lines) of 100µM LUVs made of POPE/POPG (3:1 mol/mol) 1% PEG-PE or POPC at 310 K; Abbreviations: POPE for 1-palmitoyl-2-oleoyl-*sn*-glycero-3-phosphoethanolamine, POPG for 1-palmitoyl-2-oleoyl-*sn*-glycero-3-phospho-(1'-*rac*-glycerol)

The CD spectra of peptoid **A-3** in aqueous buffer showed a curve with two negative Cotton effects at 202 and 222 nm (Figure 3A) which is the typical PolyProline I-type helix CD signature of peptoid oligomers featuring (*S*)-1-phenyl ethyl side chains.[12, 15] Upon adding large unilamellar vesicles (LUVs) made of 1-palmitoyl-2-oleoyl-*sn*-glycero-3-phosphoethanolamine (POPE)/ 1-palmitoyl-2-oleoyl-*sn*-glycero-3-phospho-(1'-*rac*-glycerol) (POPG) (3:1 mol/mol) and 1% PEGylated phosphatidylethanolamine (PEG-PE) lipid a further increase in the negative Cotton effect around 222 nm with a slightly red-shifted minima was observed suggesting a higher degree of helicity upon membrane association. The addition of PEG-PE was necessary to reduce vesicle agglutination which interferes with optical spectroscopies.[30] Related CD spectral changes were also observed upon addition of POPC LUVs but without the red shift previously observed with the bacterial membrane model. The same changes on CD signature in presence of model membranes was also reported for dodecamers studied by the Seo group.[20] These results suggest that peptoid **A-3** interacts with both model membranes but not in the same way.

In contrast, the CD spectra of the peptoid **C-9** showed only minimal changes upon lipid addition (Figure 3B). Without the lipids, this peptoid also exhibited the spectral features indicative of PPI-type helical secondary structure. However, when addition of 100 µM LUVs made from POPE/POPG (3:1 mol/mol) 1%PEG-PE or of POPC, respectively, resulted in only small changes of the molar ellipticity at 222 nm. The observed spectral changes can be explained with scattering artifacts in the presence of a high concentration of the lipids. These observations suggest that the peptoid **C-9** does not undergo conformational changes when binding to either of the model membranes.

Membrane disruption study using a calcein release assay. Fluorescence dye release experiments were conducted to evaluate the membrane disruptive properties of the selected peptoids **A-3** and **C-9** (Figure 4).

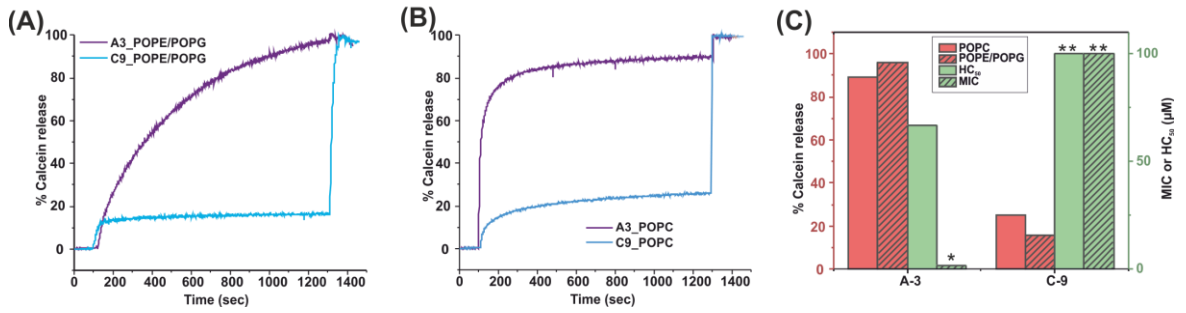

Figure 4. Percent Calcein released from LUVs made of (A) POPE/POPG (3:1) and (B) POPC after addition of peptoids peptoid **A-3** and peptoid **C-9**. (C) Correlation of % calcein release with minimum inhibitory concentration (MIC, *S. aureus*) and HC_{50}. The experiments were done at 310 K. *$MIC_{S.a}$ = 1.6 µM. **Values > 100 µM

For the study against the bacterial model membrane, calcein-loaded LUVs made of POPE/POPG (3:1 mol/mol) were used. Likewise, for the eukaryotic model membrane, POPC LUVs loaded with calcein were prepared. To compare the activities of the peptoids, for each model membrane a specific concentration of the peptoids was selected, which revealed a clear difference between them. For studies with POPE/POPG (3:1), the peptoids were added to reach a total peptoid/lipid ratio of 30 wt%. POPC LUVs were treated with 10 mol% of the peptoids. These conditions were chosen to best reveal differences between peptoids when interacting with the membranes of different composition. Initially, the LUVs of the POPE/POPG (3:1) or POPC in buffer were added to the cuvette and their fluorescence

intensity was recorded. At t = 100 sec, peptoid **A-3** was added to the cuvette containing the POPE/POPG (3:1) LUVs. A gradual increment in the fluorescence intensity was observed reaching about 96% until Triton was added at t = 1300 secs, showing a sustained **A-3**-induced release profile. However, the release profile against POPC LUVs was different. In this case, 10 mol% of **A-3** was added, which resulted in a sharp increase in the fluorescence intensity within a few seconds. **A-3** was able to release 89 % of the calcein from POPC LUVs. A similar experiment was also done for peptoid **C-9**. Addition of 30 weight % of peptoid **C-9** induced only 16 % of calcein to leak from POPE/POPG LUVs and addition of 10 mol% of this peptoid released about 25 % of the calcein from POPC LUVs. The nature of the increase in the fluorescence intensity upon treatment with peptoids was similar for both model membranes, unlike in the case of peptoid **A-3**.

The biophysical data was then compared with biological results like MIC and HC_{50}. Interestingly, peptoid **A-3** showed a high propensity to inhibit the growth of *S. aureus* with a MIC of 1.6 µM which correlates well with 96% leakage of calcein encapsulated in POPE/POPG (3:1) LUVs. Thus, the peptoid is highly active in antimicrobial assays and at the same time causes significant membrane disruption. The data against human red blood cells (HC_{50}) was also found to be corroborating with high calcein release from POPC LUVs. Indeed, peptoid **A-3** displayed toxicity against erythrocytes already at 67 µM while the release from the vesicles was recorded to be 89%. The higher toxicity was explained by the membrane-perturbing nature of peptoid **A-3**. On the other hand, peptoid **C-9**, is nontoxic (HC_{50} > 100 µM) and non-active in antimicrobial assays (MIC against *S.aureus* > 100 µM) in agreement with poor activity also in the biophysical experiments. Thereby, the membrane activity of these peptoids correlated well with their activities in biological assays.

DISCUSSION

Unlike peptides, the folding propensity of peptoids is not governed by intramolecular hydrogen bonding along the backbone but by an addition of weak backbone-side chain interactions and also sometimes side chain-side chain interactions.[9] To favor the structuration of peptoids into a PolyProline

I-like helix, specific side chains inducing *cis* conformation of the backbone *N*,*N*-disubstituted amides were developed.[24] In this study, the peptoid oligomers were designed to adopt a preferred PolyProline I-like helical structure with an amphipathic character by using *cis*-directing side chains in the whole sequence. Indeed, by contrast with cationic side chains employed in the literature to develop amphipathic cationic antimicrobial peptoids,[16] the triazolium-type side chains have the ability to enforce the *cis* amide conformation through $n \rightarrow \pi^*_{Ar}$ electronic interactions.[25]

Diversity of the triazolium-type side chains. To act as hydrophobic groups, the moderately *cis*-inducing (*S*)-1-phenylethyl side chain (spe), commonly employed to design PPI-type helical peptoids with antimicrobial properties, was used to construct oligomers constituting four series named **A**, **B**, **C** and **D**. Comparison of these four series makes it possible to examine the impact of triazolium-type side chains (nature and content). The evaluation on the panel of bacterial strains shows that the triazolium groups play a major role in the antimicrobial activity since oligomers comprised of uncharged triazole groups were completely inactive. One might think that this is only due to the absence of cationic charges but oligomers with the same design but incorporating *N*-(4-amino-butyl) glycine (*N*Lys) residues, *i.e.* ammonium groups instead of triazolium groups, start to be active at the nonamer length.[13] Here, the studied triazolium-based hexamers such as **A-2**, **B-6** and **D-13** show already interesting activities (MIC 1.6 or 3.2 μM on *S. aureus*) (Table 2). A specific antibacterial activity on *S. aureus* is highlighted for hexamers **A-2** and **B-6** since no or very low activity was detected on other tested bacterial strains, fungi and revealed nontoxic on human red blood cells (Table 2 and 3). By contrast, the hexamer **D-13** had a broad spectrum of activity on bacteria, strong activity against the three tested fungi (MIC 3.1 μM on *C. albicans* and *C. neoformans*) and also high hemolytic activity (HC_{50} 10.3 μM). The only hexamer having no activity is peptoid **C-9** for which additional positive charges (ammonium groups) were present, indicating that this high charge/length ratio of 2:3 instead of 1:3 is detrimental for the antibacterial and antifungal activities. Hexamer **C-9** was also nontoxic on the whole panel of human cells. These results on hexapeptoids show that the nature of the substituents in position 1 of the 1,2,3-triazoliums has a great impact on the selectivity profile. The lipidation of linear

peptoids was previously used as a tool to access shorter peptoid sequences with good antifungal profiles.[31] In these triazolium-based peptoids, the introduction of a lipophilic tail on the triazoliums as a sort of lipopeptide mimetics, makes the peptoid oligomers active on the panel of fungi but also very toxic on human cells (D series). The introduction of an ammonium group to mimic a lysine side chain makes the peptoid totally inactive. Benzyl and cyclohexylmethyl substituents lead to oligomers with similar activity profile but H-*N*btm$^+$-*N*spe-*N*spe-*N*btm$^+$-*N*spe-*N*spe-NH_2 **B-6** was slightly more selective against *S. aureus* and less toxic on human cells suggesting that benzyl is the best substituent in position 1 of the triazolium groups.

Aromatic versus aliphatic side chain as hydrophobic group. Starting from the series **B**, the **E** series was designed by replacing the aromatic (S)-phenylethyl side chain (*spe*) by the aliphatic (S)-tert-butyl ethyl side chain (*stbe*). Previous work from our group revealed that the *stbe* side chain is a powerful nonaromatic *cis*-inducer leading to robust PPI-type helical secondary structure[32] but it has never been used for the design of antimicrobial peptoids. Therefore, this side chain could make it possible to improve the folding homogeneity while reducing the quantity of aromatic groups. Indeed, a high content of the aromatic side chains, generally employed to improve structuration into helix, might be an obstacle in terms of physicochemical properties in a drug discovery context.[33] Satisfyingly, the hexamer **E-15** proves to be slightly more potent on *S. aureus* strains than the hexamer **B-6** (MIC 1.6 versus 3.2 µM) with a very good selectivity index ($HC_{50}/MIC_{S.a}$) of 42.9. Overall, hexamers **B-6** and **E-15** show the same activity profile, however, **E-15** is slightly more toxic on the panel of human cells than **B-6**. These results suggest that the use of chiral aromatic or aliphatic α-substituted side chains has no dramatic impact on the potency and selectivity.

Optimization of the sequence length. As a general trend, increasing the sequence length while keeping the same charge/length ratio (1:3), slightly improves the activity against *S. aureus* but leads to broader spectrum of activity on both Gram-positive and Gram-negative bacteria and also on fungi (Table 2 and 3) but unfortunately is also associated with an increase in toxicity on human cells. The selectivity index

of the nonamers thus drops to a value below 5, except for the nonamer **B-8** which has a selectivity ratio above 20 (Table 2). As previously noticed, the C series shows a different behavior. The nonamer **C-10** was inactive on Gram-positive and Gram-negative bacterial strains, slightly active on one fungus ($MIC_{\textit{C. neoformans}}$ 12.5 µM) and nontoxic at 100 µM. A further increase in the sequence length furnishes the mildly active dodecamer **C-12** but with a broad spectrum of activity across bacteria and fungi. However, these activities are not linked to the triazolium moieties since the triazolyl-based dodecamer **C-11** has the same activity profile.

To improve potency while keeping a good selectivity profile, it could be beneficial to slightly increase the cationic/hydrophobic ratio by introducing an additional cationic residue at the *C*-terminal position.[15] Applying this design, the heptamers **A-3**, **B-7** and **E-16** reveal as potent on the bacterial strains but less toxic than the nonamers (Table 4, Figure 5). This design appears to be the best compromise between activity and selectivity. One exception is the heptamer **D-14** for which a very high level of toxicity was observed confirming the detrimental effect of the lipophilic substituent on triazoliums. If both oligomers **B-7** and **E-16** show a HC_{50} on hRBC superior to 100 µM, the evaluation on the panel of human cells highlights the safer profile of heptamer **B-7** (Figure 5). This trend is not directly visible from hemolytic activity and demonstrates that it is very important to evaluate antimicrobial compounds on various cells to better appreciate their therapeutic potential. Besides, a significant variation in cell susceptibility could be observed for heptamer **A-3** which was found to be more toxic for HaCaT skin cells, while the other peptoids **B-7** and **E-16** did not have higher toxicity on these cells.

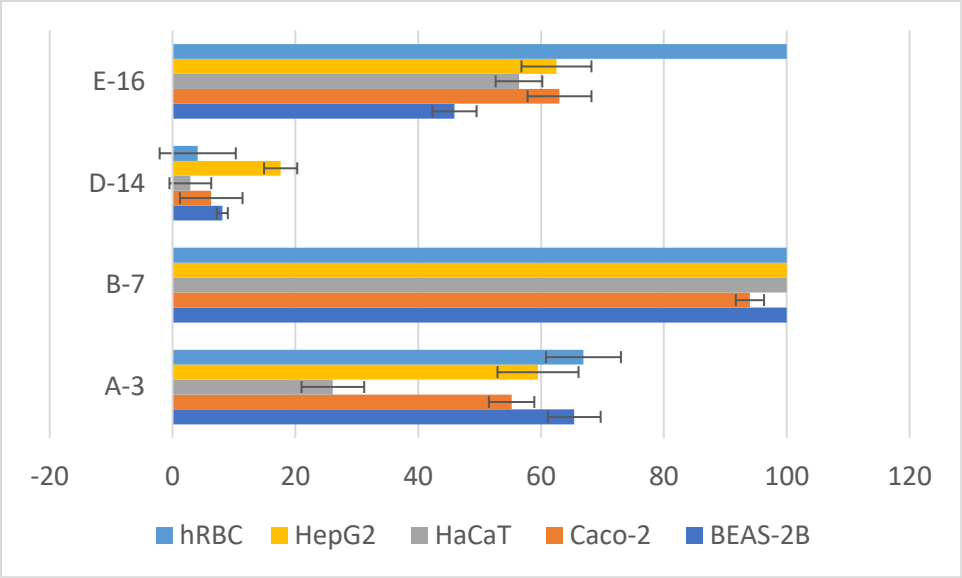

Figure 5. Comparison of the cytotoxic concentrations on human cell panel (CC_{50} in µM) and the hemolytic activity (HC_{50} in µM) for all heptameric peptoids.

Investigation of the Mechanisms of action. Antimicrobial peptides (AMPs) are key players in host defenses, operating as antimicrobial agents and also modulators of the inflammatory response. The mechanisms of action of cationic amphipathic antimicrobial peptides are well described by the SMART model (Soft Membranes Adapt and Respond, also Transiently, to external stimuli) where the amphipathic nature of their 3D structures results in the partitioning into the membrane interface.[34] In this configuration the peptides/peptoids take considerably more space at the level of the lipid headgroups when compared to the membrane interior, which results in extensive curvature strain, membrane thinning and the destabilization of the bilayer packing. At increasing peptide/peptoid concentrations membrane openings and also membrane rupture are observed.[35] In-line with this mode, most of the previously developed antimicrobial linear peptoids were shown to lyse bacteria through cell membrane disruption.[16] It was also suggested that some particular linear peptoids could also operate intracellularly.[36] According to the circular dichroism study, our triazolium-grafted oligomers show very similar conformational changes in presence of the bacterial membrane model than those induced by antibacterial peptoids developed by Barron and Seo.[12,20] This suggest that the same types of interaction are involved for these two classes of cationic peptoids. Besides, the calcein release assay clearly show that the active peptoid has a disruptive effect on the membrane model

while the inactive peptoid has no deleterious effect. In analogy to peptides, the different degree and kinetics of calcein release are probably related to the membrane curvature strain caused by peptoid insertion.[35] These biophysical studies strongly support that the bactericidal effect of these triazolium-grafted peptoids is primarily due to the disruption of the bacterial membrane. This also explains why these compounds are more active on Gram-positive than on Gram-negative pathogens. Moreover, it can be hypothesized that the antifungal activity observed for some of the triazolium-grafted peptoids (*i.e.* nonamers **A-5**, **B-8**, **E-17** and **D** series; Table 3) also involves membrane disruption because of the poor selectivity observed. Indeed, since fungi and human cells share similar membrane composition, achieving antifungal selectivity is challenging for membrane-active compounds. By contrast, the selectivity profile of oligomers with high cationic content (*i.e.* **C-10** and **C-12**; Table 3) suggests the involvement of another mechanism of action on fungi (selectivity ratio: $MIC_{\textit{C. neoformans}}$ /HC_{50} > 10).

A number of AMPs have shown ability to regulate inflammation to promote immune homeostasis.[37] One mechanism is the inhibition of endotoxin-induced production of pro-inflammatory cytokines by interacting with endotoxin such as lipopolysaccharide (LPS) from Gram negative bacteria or lipoteichoic acid (LTA) from Gram positive bacteria. Recently, a cationic peptoid exhibiting an LPS-scavenging activity similar to that of the lipopeptide polymyxin E was reported.[38] Therefore, the anti-inflammatory activity of these triazole/triazolium-grafted peptoids was assessed by evaluating their ability to block the pro-inflammatory effect induced by lipopolysaccharide (LPS) or lipoteichoic acid (LTA). Unfortunately, the toxicity of peptoids on the murine macrophage used in this test sometimes prevents us from concluding on the anti-inflammatory activity of certain compounds (*i.e.* nonamers **A-5**, **B-8** and **E-17,** hexamer **D-13** and heptamer **D-14**; Figure 2). However, it was still possible to highlight anti-inflammatory activities similar to those of the polymyxin B reference. Notably, the uncharged nonamer **A-4** that is totally inactive on bacteria and fungi, inhibits selectively the inflammation caused by LTA from *S. aureus* (IC_{50} ~ 20 µM). More interestingly, the heptamers **B-7** and particularly **E-16** that were found to have the best therapeutic profiles (Figure 5), appear to regulate inflammation caused by LPS or LTA.

To conclude, the present study has enabled to evaluate the spectrum of activity on bacteria and fungi of this new class of triazolium-grafted linear peptoid oligomers. The combination of evaluation on bacteria, fungi and human cells panel and the careful modulation of several parameters: nature of the triazolium side chains, charge content, nature and content of hydrophobic/lipophilic side chains, sequence design and length, have led to optimized compounds with improved selectivity profile to fight *S. aureus* pathogens. Five oligomers reach a selectivity index (SI = $HC_{50}/MIC_{S.a}$) above 30. In particular, the results highlight the great potential of heptamers **B-7** and **E-16** comprising three *N*btm$^+$ triazolium residues and four aromatic *Nspe* or aliphatic *Nstbe* as hydrophobic residues. Regarding the mechanism of action, it is noteworthy from biophysical studies in presence of bacterial membrane model that this class of antimicrobial peptoids primarily act by membrane disruption. Indeed, a direct correlation was observed between antibacterial activity and oligomer conformational change upon contact with model membrane as well as bacterial model membrane disruption. However, additional intracellular targets cannot be totally excluded for short oligomers (hexamers and heptamers). Interestingly, the triazolium-grafted oligomers with good selectivity profile (*i.e.* heptamers **B-7** and **E-16**) were also found to have anti-inflammatory activity. The combination of anti-inflammatory and antimicrobial activities is particularly interesting for the development of new effective treatments in the management of chronic wound infections.[39,40] The present findings further demonstrate the potential of these triazolium-grafted peptoids as antimicrobials and have enable to find the best design and the right cationic/hydrophobic balance to selectively target *S. aureus* bacterial strains. Further studies are ongoing to evaluate the ability of these peptidomimetics to target bacteria evolving in difficult-to-treat lifestyles such as biofilm or intracellular reservoir.

MATERIALS AND METHODS

Peptoid synthesis and characterization. All solvents and chemicals obtained from commercial sources were used without further purification. Protocols for the solid-phase synthesis and oligomers

characterization are described in the supplementary materials. NMR spectra were recorded on a 400 MHz Bruker AC 400 spectrometer. HRMS was recorded on a Micromass Q-Tof Micro (3000 V) apparatus or a Q Exactive Quadrupole-Orbitrap Mass Spectrometer. LC-MS was recorded a Q Exactive Quadrupole-Orbitrap Mass Spectrometer coupled to a UPLC Ultimate 3000 (Kinetex EVO C18; 1,7µm; 100mm x 2,1mm column with a flow rate of 0.45 ml.min-1 with the following gradient: a linear gradient of solvent B from 5% to 95% over 7.5 min (solvent A = H2O + 0.1% formic acid, solvent B = acetonitrile + 0.1% formic acid) equipped with a DAD UV/VIS 3000 RS detector). Preparative HPLC was performed on a Varian instrument equipped with a C18 Varian Dynamax Microsorb 60-8 column (C18, 8 µm, 60 Å, 250 mm × 41.4 mm).

Bacterial strains. Antimicrobial evaluations were performed on the panel of bacterial strains listed in Table 5.

Table 5. List of the bacterial strains studied

Strain	**Description**	**Growth conditions**	**Origin**
Escherichia coli	JM109	Mueller Hinton, 37°C	our lab
Escherichia coli	ATCC25922 FDA strain Seattle 1946	Mueller Hinton, 37°C	ATCC
Enterococcus faecalis	ATCC29212 strain Portland	Mueller Hinton, 37°C	ATCC
Pseudomonas aeruginosa	ATCC27853 strain Boston	Mueller Hinton, 37°C	ATCC
Staphylococcus aureus	CIP65.25, strain 64-002	Mueller Hinton, 37°C	CRBIP

Antimicrobial activity. The Minimal Inhibitory Concentrations (MIC) were determined by antimicrobial susceptibility testing according to The European Committee on Antimicrobial Susceptibility Testing - EUCAST. In brief, overnight bacteria cultured in Mueller Hinton (MH) medium were diluted at 1:100 in fresh MH and cultured at 37°C with shaking at 200 rpm to an optical density at 600 nm of 0.5. Then, 50 µL of 2 × 106 CFU/ml was added into each well of a 96-well microtiter polystyrene tray with 50 µL MH of a series of 2-fold dilutions of the peptoid to be tested. The mixtures were incubated at 37°C for 18 h. MIC was defined as the lowest antibiotic concentration that inhibited visible bacterial growth. To

determine the Minimal Bactericidal Concentrations (MBC), aliquots (5 µL) representing the MIC and all the more concentrated test dilutions were plated and enumerated to determine viable cells, *i.e.* Colony Forming Unit (CFU)/ml. The MBC was defined as the lowest concentration that demonstrates a pre-determined reduction (such as 99.9%) in CFU/ml when compared to the MIC dilution. Experiments were conducted in triplicate (n = 3).

Antifungal activity. The antifungal effect of peptoids was tested following the reference methods for yeasts (NCCLS M27-A) and molds (M38-P) as previously described.[41] Liquid suspension of the yeasts *Candida albicans* (DSM 10697) and *Cryptococcus neoformans* (DSM11959) were prepared by resuspending colonies collected from PDA plates in sterile NaCl 0.9% solution. Yeasts were then diluted at 1–2 × 10^3 yeasts/mL in RMPI media buffered with MOPS (final concentration of 0.165 mol/L (pH 7.0)). For filamentous fungi, conidi were collected from *Aspergillus fumigatus* (DSM 819) grown on PDA plates using sterile solution of NaCl 0.9% supplemented with Tween at 0.1%. After counting under microscope, dilution at 2–3 × 10^4 conidi/mL were prepared in RMPI media buffered with MOPS (final concentration of 0.165 mol/L (pH 7.0)). Diluted yeast or fungi were then subjected to MIC testing in 96-wells plates. Plates were incubated at 35°C for 24-48 h before reading. At the end of the incubation, the MIC values were determined as the lowest concentrations of drug that completely inhibited visible growth of the organism. Experiments were conducted in duplicate (n = 2). At the end of the MIC assays, Minimum Fungicidal Concentrations (MFC) were determined by plating 20 µL from each well on PDA agar. After 48 h incubation at 35°C, MFC were determined as the concentrations of peptoids for which no fungal growth was observed.

Hemolytic activity. The ability of the peptoids to cause hemolysis was evaluated using human erythrocytes from whole blood as previously described.[42] Briefly, fresh human red blood cells (RBC) (Divbio Science Europe, NL) were washed 3 times with sterile phosphate buffer saline (PBS, pH 7.4) and collected by centrifugation at 800 × g for 5 min. The RBC were then resuspended in DMEM without phenol red supplemented with 10 % fetal bovine serum to a final concentration of 8%. 100 µL of human

RBC were then added to sterile 96 well microplates already containing serial dilutions of the peptoids in 100 µL of media. After 1 h at 37°C, the RBC were centrifuged at 800 g for 5 min and the supernatant (100 µL) was carefully transferred to new 96 well microplates. The absorbance at 450 nm was measured using a microplate reader (SynerMix, Biotek). Triton-X100 at 0.1% (v/v) was used as positive control giving 100% hemolysis. The hemolysis caused by peptoids was expressed as percentage of total hemolysis and the HC_{50} values (i.e. the concentration of peptoids causing 50% of hemolysis) were calculated using GraphPad® Prism 7 software. Experiments were performed in triplicate (n=3).

Cytotoxicity. Toxicity of peptoids was tested as previously described[28] using the following cell types: BEAS-2B (normal human airway epithelial cells), Caco-2 (human intestinal cell line), HaCaT (normal human keratinocytes), and HepG2 (human liver cell line). Cells were cultured in Dulbecco's modified essential medium (DMEM) supplemented with 10% fetal calf serum (FCS), 1% L-glutamine and 1% antibiotics (all from Invitrogen). Cells were routinely grown onto 25 cm^2 flasks maintained in a 5% CO_2 incubator at 37°C. Briefly, cells grown on 25 cm^2 flasks were detached using trypsin-EDTA solution (Thermofisher) and seeded into 96-well cell culture plates (Greiner Bio-one) at approximately 10^4 cells per well (counted using Mallasez's chamber). The cells were grown at 37°C in a 5% CO_2 incubator until they reached 80-90 % confluence (approximately 24-48 h of seeding). Wells were then aspirated and increasing concentrations of peptoids were added to the cells and incubated for a further 48 h at 37°C in a 5% CO_2 incubator. The wells were then emptied, and cell viability was evaluated using resazurin based *in vitro* toxicity assay kit (Sigma-Aldrich) following manufacturer's instructions. Briefly, resazurin stock solution was diluted 1:10 in sterile PBS containing calcium and magnesium (PBS^{++}, pH 7.4) and emptied wells were filled with 100 μL of the resazurin diluted solution. After 1 h incubation at 37°C with the peptide treated cells, fluorescence intensity was measured using a microplate reader (SynerMix, Biotek, Ex 530 nm/Em 590 nm). The fluorescence values were normalized by the controls and expressed as the percentage of cell viability. The CC_{50} values of peptoids on cell viability (i.e. the concentration of peptoids causing a reduction of 50% of the cell viability) were calculated using GraphPad® Prism 7 software. Experiments were performed in triplicate (n=3).

Anti-inflammatory activity. The inhibitory activity of peptoids and comparator compound (polymyxin B, PMB) against lipopolysaccharide (LPS) and lipoteichoic acid (LTA) was assessed using eLUCidate™ Raw 264.7 NF-κB reporter cell line (AMSBIO) as previously described.[29] Briefly, cells were grown and maintained following manufacturer's instructions in Dulbecco's modified essential medium (DMEM) supplemented with 10 % fetal calf serum (FCS), 1 % L-glutamine, 1% antibiotics (Invitrogen) and containing 3 μg/mL of puromycin (Sigma-Aldrich). To test the inhibitory activity of peptoids on LPS or LTA-drived NF-κB activation, eLUCidate™ Raw 264.7 cells grown on 75 cm^2 flasks were detached using trypsin-EDTA solution (Thermofisher) and seeded into 96-well cell culture plates (Greiner Bio-one) at approximately 25,000 cells per well (counted using Mallasez's chamber). The next day, wells were emptied and cells were exposed to 10 ng/mL of LPS from *E coli* or 10 μg/mL of LTA from *S. aureus* (Invivogen) in the presence of increasing concentrations of peptoids (from 0 to 100 μM, serial 1:2 dilutions). Polymyxin B (PMB) (Sigma-Aldrich) was used as positive control based on its well-known activity as blocker/neutralizer of LPS and LTA. After 6 h incubation at 37°C and 5% CO_2, wells were emptied and the cells were treated with 70 μL of ice-cold PBS containing 1% Triton X-100. After 10 min incubation on ice under orbital shaking at 200 rpm, 50 μL of cell lysates were collected and transferred into white 96-well luminescence plates (Dominique Dutscher) already containing 100 μL of Renilla luciferase substrate (Yelen). Luminescence signals of the wells were immediately measured using microplate reader (SynerMix, Biotek). The luminescence values were expressed as percentage of control inflammation corresponding to values obtained after treatment with LPS or LTA in the absence of inhibitor. The IC_{50} values of peptoids and PMB on LPS or LTA-mediated inflammation (*i.e.* the concentration of molecule causing a reduction of 50 % of the luciferase's induction caused by LPS or LTA) were calculated using GraphPad® Prism 7 software. Experiments were performed in triplicate (n=3).

Materials for large unilamellar vesicles. The phospholipids 1-palmitoyl-2-oleoyl-*sn*-glycero-3-phosphoethanolamine (POPE), 1-palmitoyl-2-oleoyl-*sn*-glycero-3-phospho-(1'-rac-glycerol) (sodium salt) (POPG), 1-palmitoyl-2-oleoyl-*sn*-glycero-3-phosphocholine (POPC) and 1,2-distearoyl-*sn*-glycero-

3-phosphoethanolamine-N-[methoxy(polyethylene glycol)-2000] (ammonium salt) (PEG2000 PE) were purchased from Avanti Polar Lipids (Birmingham, AL). Bis[N, N−bis(carboxymethyl)aminomethyl]fluorescein (Calcein) was from Sigma/Merck KGaA (Darmstadt, Germany).

Preparation of liposomes for the circular dichroism (CD) spectroscopy studies. CD experiments were performed for both bacterial (POPE/POPG (3:1, mol/mol) with 1% PEG2000 PE) and eukaryotic (POPC) model membranes. Large unilamellar vesicles 100 nm in size were used for the studies. The respective lipid mixtures were co-dissolved in chloroform/methanol (2:1, v/v). After completely solubilizing, the solvent mixture was removed by exposing the content to the stream of nitrogen gas, followed by exposing the vial to the high vacuum of a lyophilizer (1 mbar) for overnight to ensure the removal of solvent traces. The resulting lipid film was rehydrated with 10 mM Tris buffer (pH= 7). The lipids were then subjected to 3 vortex-freeze-thaw cycles. The resultant mixture was then extruded (mini extruder Avanti Polar Lipids, Alabaster, AL, USA) by passing through a polycarbonate membrane with a pore size of 100 nm diameter (Whatman Nucleopore Track-Etch Membrane; Little Chalfont, UK).

Circular dichroism spectroscopy. A JASCO J-810 spectropolarimeter (Tokyo, Japan) equipped with Peltier JASCO temperature control system-PFD-425S (Tokyo, Japan) was used to record the CD measurements at 310 K. A 10 µM peptoid solution was prepared from their respective stocks using 10 µM Tris pH 7. Initially, the CD spectra of the peptoid alone were obtained, followed by the subsequent addition of the LUVs of POPE/POPG (3:1)/1% PEG-PE (100 µM, for the bacterial model membrane study) and the same of POPC (100 µM, for the eukaryotic model membranes) to maintain a compound-to-lipid ratio of 1/10. All the analyses were recorded between 190 to 250 nm in a cuvette of 10 mm path length. Four acquisitions were made for individual experiments with a bandwidth of 3.00 nm and step resolution of 1 nm. The step scan method was employed for individual readings using an adaptive integration time of 1-8 seconds. The data were obtained as mdeg, which was then used to calculate the molar ellipticity.

Molar ellipticity (deg.cm^2.dmol^{-1}) = [Ellipticity (m.deg) * 10^6] / [path length (mm) *peptoid (μM). n where n = number of amide bonds in the peptoid.

Noise of the data was removed using Adjacent- averaging smoothening (Origin 2019b)

Preparation of calcein-loaded liposomes for the calcein release fluorescence experiments. Large unilamellar vesicles (LUVs) loaded with calcein were used for this experiment by first dissolving POPE/POPG (3:1, mol/mol) or POPC in chloroform/methanol (2:1, v/v). The solvents were removed by evaporating them under a stream of nitrogen gas and kept in the vacuum of the lyophilizer for 24 h. The resultant lipid films on the glass vial were then hydrated with 50 mM Tris (pH=7) and 50 mM calcein disodium salt. The entire mixture was subjected to repeated cycles of vortexing-freeze-thaw (4 cycles) and then extruded (17 times, mini extruder Avanti Polar Lipids, Alabastar, AL, USA) through membranes with a pore size of 400 nm diameter (Whatman Nucleopore Track-Etch Membrane; Little Chalfont, UK). The dye outside the vesicles was removed by gel filtration through a Sephadex G50 column (Steinheim, Germany) using buffer of 50 mM Tris supplemented with 50 mM NaCl to compensate for the osmotic change caused by the calcein and its sodium counter ions. The column-purified vesicles were then collected in several fractions, and their respective phospholipid concentrations were determined by phosphate analysis.[43] For the studies with POPE/POPG (3:1), the compound/lipid (C:L) ratio was maintained at 30 weight%. The C:L for the studies with POPC was kept at 10 mol%. For each membrane system, the peptoid to lipid ratio was chosen according to the biggest expected differentiation between the molecules. In this way the dye release at the single peptoid to lipid ratio reflects the shift of the critical concentration for dye release.

Calcein release fluorescence experiments. The following study was conducted by measuring the fluorescence intensity of the dye, Calcein, leaking from the LUVs upon peptoid addition. This was measured by a Fluoromax-Plus spectrofluorometer (HORIBA Scientific, Kyoto, Japan), and the experiments were conducted at 313 K.

For the studies on bacterial model membranes, 500 µM LUVs of POPE/POPG (3:1) were added to the cuvette containing 1 mL of 50 mM Tris, 50 mM NaCl. Then at t = 100 sec, 30 weight% of the respective peptoids were injected. The leakage of the dye was observed for the next 1200 sec, and then the experiment was terminated by adding the positive control (Triton at t = 1300 sec). The excitation wavelength was 485 nm, and the intensity of the fluorescence (I) was recorded at 515 nm. The percentage of the calcein released from the LUVs was then calculated as

$$I\% = (I - I_0) / (I_{max} - I_0) * 100$$

where I_0 is the intensity observed before the peptoid addition, and the I_{max} is the intensity observed upon the addition of 10 µL of 10 % Triton X-100 (fully disrupted vesicles).

Acknowledgements

This work was supported by the project AmphiPep ANR-20-CE18-0021-01 and by the French Government IDEX-ISITE initiative 16-IDEX-0001 (CAP 20-25 Emergence) for Clermont Auvergne University. The financial contributions of the Indo-French Centre for the Promotion of Advanced Research (IFCPAR/CEFIPRA) (project no. 62T10-1), the Agence Nationale de la Recherche (Naturalarsenal 19-AMRB-0004-02, SAFEST 21-CE18-0043), the Interdisciplinary Thematic Institute SysChem, *via* the IdEx Unistra (ANR-10-IDEX-0002), the région Auvergne-Rhône-Alpes and the Région Grand-Est are also gratefully acknowledged.

---

[1] Zasloff, M. Antimicrobial peptides of multicellular organisms. *Nature* **2002**, *415*, 389–395. DOI: 10.1038/415389a

[2] Brogden, K. Antimicrobial peptides: pore formers or metabolic inhibitors in bacteria? *Nat. Rev. Microbiol.* **2005**, *3*, 238–250. DOI: 10.1038/nrmicro1098

[3] Guilhelmelli, F.; Vilela, N.; Albuquerque, P.; Derengowski Lda, S.; Silva-Pereira, I.; Kyaw, C. M. Antibiotic development challenges: the various mechanisms of action of antimicrobial peptides and of bacterial resistance. *Front. Microbiol.* **2013**, *4*, 353. DOI: 10.3389/fmicb.2013.00353

[4] Sarkar, T.; Chetia, M.; Chatterjee, S. Antimicrobial Peptides and Proteins: From Nature's Reservoir to the Laboratory and Beyond. *Front. Chem.* **2021**, *9*, 691532. DOI: 10.3389/fchem.2021.691532

[5] Tew, G. N.; Scott, R. W.; Klein, M. L.; DeGrado W. F. De Novo Design of Antimicrobial Polymers, Foldamers, and Small Molecules: From Discovery to Practical Applications. *Acc. Chem. Res.* **2010**, *43* (1), 30–39. DOI: 10.1021/ar900036b

[6] Yokoo, H.; Hirano, M.; Misawa, T.; Demizu, Y. Helical Antimicrobial Peptide Foldamers Containing Non-proteinogenic Amino Acids. *Chem. Med. Chem.* **2021**, *16* (8), 1226-1233. DOI: 10.1002/cmdc.202000940

[7] Bechinger, B. Structure and Functions of Channel-Forming Peptides: Magainins, Cecropins, Melittin and Alamethicin. *J. Membrane Biol.* **1997**, *156*, 197–211. DOI: 10.1007/s002329900201

[8] Bechinger, B.; Juhl, D.W.; Glattard, E.; Aisenbrey, C. Revealing the Mechanisms of Synergistic Action of Two Magainin Antimicrobial Peptides. *Front. Med. Technol.* **2020**, *2*, 615494. DOI: 10.3389/fmedt.2020.615494

[9] Sang, P.; Cai, J. Unnatural helical peptidic foldamers as protein segment mimics. *Chem. Soc. Rev.* **2023**, *52* (15), 4843-4877. DOI: 10.1039/D2CS00395C

[10] Yang, W.; Seo, J.; Kim J. H. Protein-mimetic peptoid nanoarchitectures for pathogen recognition and neutralization. *Nanoscale* **2023**, *15*, 975-986. DOI: 10.1039/D2NR05326H

[11] Patch, J. A.; Barron A. E. Helical Peptoid Mimics of Magainin-2 Amide. *J. Am. Chem. Soc.* **2003**, *125* (40), 12092-12093. DOI: 10.1021/ja037320d

[12] Chongsiriwatana, N. P.; Patch, J. A.; Czyzewski, A. M.; Dohm, M. T.; Ivankin, A.; Gidalevitz, D.; Zuckermann, R. N.; Barron, A. E. Peptoids that mimic the structure, function, and mechanism of helical antimicrobial peptides. *Proc. Natl. Acad. Sci. U.S.A.* **2008**, *105* (8), 2794-2799. DOI: 10.1073/pnas.0708254105

[13] Bolt, H. L.; Eggimann, G. A.; Jahoda, C. A. B.; Zuckermann, R. N.; Sharples, G. J.; Cobb, S. L. Exploring the links between peptoid antibacterial activity and toxicity. *Med. Chem. Commun.* **2017**, *8* (5), 886-896. DOI: 10.1039/c6md00648e

[14] Mojsoska, B.; Zuckermann, R.N.; Jenssen, H. Structure-Activity Relationship Study of Novel Peptoids That Mimic the Structure of Antimicrobial Peptides. *Antimicrob. Agents Chemother.* **2015**, *59* (7), 4112–4120. DOI:10.1128/AAC.00237-15

[15] Lee, J.; Kang, D.; Choi, J.; Huang, W.; Wadman, M.; Barron, A. E.; Seo, J. Effect of side chain hydrophobicity and cationic charge on antimicrobial activity and cytotoxicity of helical peptoids. *Bioorg. Med. Chem. Lett.* **2018**, *28* (2), 170–173. DOI: 10.1016/j.bmcl.2017.11.034

[16] Bicker, K. L.; Cobb, S. L. Recent advances in the development of anti-infective peptoids. *Chem. Commun.* **2020**, *56* (76), 11158-11168. DOI: 10.1039/D0CC04704J

[17] Molchanova, N.; Nielsen, J.E.; Sørensen, K.B.; Prabhala, B. K.; Hansen, P. R.; Lund, R.; Barron, A. E.; Jenssen, H. Halogenation as a tool to tune antimicrobial activity of peptoids. *Sci. Rep.* **2020**, *10*, 14805. DOI: 10.1038/s41598-020-71771-8

[18] Lin, J. S.; Bekale, L. A.; Molchanova, N.; Nielsen, J. E.; Wright, M.; Bacacao, B.; Diamond, G.; Jenssen, H.; Santa Maria, P. L.; Barron, A. E. Anti-persister and Anti-biofilm Activity of Self-Assembled Antimicrobial Peptoid Ellipsoidal Micelles. *ACS Infect. Dis.* **2022**, 8 (9), 1823−1830. DOI: 10.1021/acsinfecdis.2c00288

[19] Huang, M.L.; Shin, S.B.; Benson, M.A.; Torres, V.J.; Kirshenbaum, K. A comparison of linear and cyclic peptoid oligomers as potent antimicrobial agents. *Chem. Med. Chem.* **2012**, *7* (1), 114-122. DOI: 10.1002/cmdc.201100358

[20] Nam, H. Y.; Choi, J.; Kumar, S. D.; Nielsen, J. E.; Kyeong, M.; Wang, S.; Kang, D.; Lee, Y.; Lee, J.; Yoon, M.-H.; Hong, S.; Lund, R.; Jenssen, H.; Shin, S. Y.; Seo, J. Helicity Modulation Improves the Selectivity of Antimicrobial Peptoids. *ACS Infect. Dis.* **2020**, *6* (10), 2732-2744. DOI: 10.1021/acsinfecdis.0c00356

[21] Shyam, R.; Charbonnel, N.; Job, A.; Blavignac, C.; Forestier, C.; Taillefumier, C.; Faure, S. 1,2,3-Triazolium-Based Cationic Amphipathic Peptoid Oligomers Mimicking Antimicrobial Helical Peptides. *Chem. Med. Chem.* **2018**, *13* (15), 1513-1516. DOI: 10.1002/cmdc.201800273

[22] Shyam, R.; Forestier, C.; Charbonnel, N.; Roy, O.; Taillefumier, C.; Faure, S. Solution-Phase Synthesis of Backbone-Constrained Cationic Peptoid Hexamers with Antibacterial and Anti-Biofilm Activities. *Eur. J. Org. Chem.* **2021**, *2021* (42), 5813-5822. DOI: 10.1002/ejoc.202101155

[23] Kirshenbaum, K.; Barron, A. E.; Goldsmith, R. A.; Armand, P.; Bradley, E. K.; Truong, K. T. V.; Dill, K. A.; Cohen, F. E.; Zuckermann, R. N. Sequence-specific polypeptoids: A diverse family of heteropolymers with stable secondary structure. *Proc. Natl. Acad. Sci. USA* **1998**, *95* (8), 4303 – 4308. DOI: 10.1073/pnas.95.8.4303

[24] Kalita, D.; Sahariah, B.; Mookerjee, S. P.; Sarma, B. K. Strategies to Control the Cis-Trans Isomerization of Peptoid Amide Bonds. *Chem. Asian J.* **2022**, *17* (11), e202200149. DOI: 10.1002/asia.202200149

[25] Caumes, C.; Roy, O.; Faure, S.; Taillefumier, C. The click triazolium peptoid side chain: a strong cis-amide inducer enabling chemical diversity. *J. Am. Chem. Soc.* **2012**, *134* (23), 9553-9556. DOI: 10.1021/ja302342h

[26] Nomenclature: *N*chtm for *N*-(1-cyclohexylmethyl-1,2,3-triazolylmethyl)glycine, *N*aetm for *N*-(1-(2-aminoethyl)-1,2,3-triazolylmethyl)glycine, *N*spe for N-(S)-(1-phenylethyl)glycine, *N*stbe for *N*-(S)-(1-tert-butylethyl)glycine, *N*chtm$^+$ for *N*-(1-cyclohexylmethyl-3-methyl-1,2,3-triazolylmethyl)glycine, Nbtm$^+$ for *N*-(1-benzyl-3-methyl-1,2,3-triazolylmethyl)glycine, Naetm$^+$ for *N*-(1-(2-aminoethyl)-3-methyl-1,2,3-triazolylmethyl)glycine and *N*otm$^+$ for *N*-(1-octyl-3-methyl-1,2,3-triazolylmethyl)glycine.

[27] Connolly, M. D.; Xuan, S.; Molchanova, N.; Zuckermann, R. N. Chapter Eight - Submonomer synthesis of sequence defined peptoids with diverse side-chains, Editor(s): E. James Petersson, Methods in Enzymology, Academic Press, Volume 656, **2021**, p. 241-270. DOI: 10.1016/bs.mie.2021.04.022

[28] Olleik, H.; Yacoub, T.; Hoffer, L.; Gnansounou, S.M.; Benhaiem-Henry, K.; Nicoletti, C.; Mekhalfi, M.; Pique, V.; Perrier, J.; Hijazi, A.; Baydoun, E.; Raymond, J.; Piccerelle, P.; Maresca, M.; Robin, M. Synthesis and Evaluation of the Antibacterial Activities of 13-Substituted Berberine Derivatives. *Antibiotics* **2020**, *9*, 381. DOI: 10.3390/antibiotics9070381

[29] Oyama, L.B.; Olleik, H.; Teixeira, A.C.N.; Guidini, M.M.; Pickup, J. A.; Yeo Pei Hui, B.; Vidal, N.; Cookson, A.R.; Vallin, H.; Wilkinson, T.; Bazzolli, D.M.S. Richards, J.; Wootton, M.; Mikut, R.; Hilpert, K.; Maresca, M.; Perrier, J.; Hess, M.; Mantovani, H.C.; Fernandez-Fuentes, N.; Creevey, C.J.; Huws, S.A. In silico identification of two peptides with antibacterial activity against multidrug-resistant *Staphylococcus aureus*. *npj Biofilms Microbiomes* **2022**, 8, 58. DOI: 10.1038/s41522-022-00320-0**.**

[30] Cummings, J. E.; Vanderlick, T. K. Aggregation and hemifusion of anionic vesicles induced by the antimicrobial peptide cryptdin-4. *Biochim. Biophys. Acta* **2007**, *1768*, 1796–1804. DOI: 10.1016/j.bbamem.2007.04.016

[31] Green, R. M.; Bicker, K. L. Discovery and Characterization of a Rapidly Fungicidal and Minimally Toxic Peptoid against Cryptococcus neoformans. *ACS Med. Chem. Lett.* **2021**, *12* (9), 1470-1477. DOI: 10.1021/acsmedchemlett.1c00327

[32] Roy, O.; Dumonteil, G.; Faure, S.; Jouffret, L.; Kriznik, A.; Taillefumier C. Homogeneous and Robust Polyproline Type I Helices from Peptoids with Nonaromatic α-Chiral Side Chains. *J. Am. Chem. Soc.* **2017**, *139* (38), 13533-13540. DOI: 10.1021/jacs.7b07475

[33] Gopalakrishnan, R.; Frolov, A. I.; Knerr, L.; Drury III, W. J.; Valeur, E. Therapeutic Potential of Foldamers: From Chemical Biology Tools To Drug Candidates? *J. Med. Chem.* **2016**, *59*, 9599-9621. DOI: 10.1021/acs.jmedchem.6b00376

[34] Bechinger, B. The SMART model: Soft Membranes Adapt and Respond, also Transiently, in the presence of antimicrobial peptides. *J. Pept. Sci.* **2015**, *21* (5), 346-55. DOI: 10.1002/psc.2729.

[35] Aisenbrey, C.; Marquette, A.; Bechinger, B. The Mechanisms of Action of Cationic Antimicrobial Peptides Refined by Novel Concepts from Biophysical Investigations. *Adv. Exp. Med. Biol.* **2019**, *1117*:33-64. DOI: 10.1007/978-981-13-3588-4_4

[36] Chongsiriwatana, N. P.; Lin, J.S.; Kapoor, R.; Wetzler, M.; Rea, J. A. C.; Didwania, M.K.; Contag, C.H.; Barron, A.E. Intracellular biomass flocculation as a key mechanism of rapid bacterial killing by cationic, amphipathic antimicrobial peptides and peptoids. *Sci Rep.* **2017**, *7*(1):16718. DOI: 10.1038/s41598-017-16180-0

[37] Mookherjee, N.; Anderson, M.A.; Haagsman, H.P; Davidson, D. J. Antimicrobial host defence peptides: functions and clinical potential. *Nat. Rev. Drug Discov.* **2020**, *19*, 311–332. DOI: 10.1038/s41573-019-0058-8

[38] Cafaro, V.; Bosso, A.; Di Nardo, I.; D'Amato, A.; Izzo, I.; De Riccardis, F.; Siepi, M.; Culurciello, R.; D'Urzo, N.; Chiarot, E.; Torre, A.; Pizzo, E.; Merola, M.; Notomista, E. The Antimicrobial, Antibiofilm and Anti-Inflammatory Activities of P13#1, a Cathelicidin-like Achiral Peptoid. *Pharmaceuticals* **2023**, *16*, 1386. DOI: 10.3390/ph16101386

[39] Steinstraesser, L.; Hirsch, T.; Schulte, M.; Kueckelhaus, M.; Jacobsen, F.; Mersch, E.A.; Stricker, I.; Afacan, N.; Jenssen, H.; Hancock, R.E.W. Kindrachuk, J. Innate Defense Regulator Peptide 1018 in Wound Healing and Wound Infection. *PLoS ONE* **2012**, *7* (8): e39373. DOI: 10.1371/journal.pone.0039373

[40] Wieczorek, M.; Jenssen, H.; Kindrachuk, J.; Scott, W.R.; Elliott, M.; Hilpert, K.; Cheng, J.T.; Hancock, R.E.; Straus, S.K. Structural studies of a peptide with immune modulating and direct antimicrobial activity. *Chem Biol.* **2010**, *17* (9):970-980. DOI: 10.1016/j.chembiol.2010.07.007

[41] Olleik, H.; Nicoletti, C.; Lafond, M.; Courvoisier-Dezord, E.; Xue, P.; Hijazi, A.; Baydoun, E.; Perrier, J.; Maresca, M. Comparative Structure–Activity Analysis of the Antimicrobial Activity, Cytotoxicity, and Mechanism of Action of the Fungal Cyclohexadepsipeptides Enniatins and Beauvericin. *Toxins* **2019**, *11*, 514. DOI: 10.3390/toxins11090514

[42] Benkhaled, B. T.; Hadiouch, S.; Olleik, H.; Perrier, J.; Ysacco , C.; Guillaneuf, Y.; Gigmes, D.; Maresca, M.; Lefay, C. Elaboration of antimicrobial polymeric materials by dispersion of well-defined amphiphilic methacrylic SG1-based copolymers. *Polym. Chem.* **2018**, *9* (22), 3127-3141. DOI: 10.1039/C8PY00523K

[43] Chen, P.S.; Toribara, T.Y.; Warner, H. Microdetermination of Phosphorus. Analytical Chemistry **1956**, *28*, 1756- 1758. DOI: 10.1021/ac60119a033